

## Ferromagnetism in an orbitally degenerate Hubbard model

J. Kuei\* and R. T. Scalettar

*Department of Physics, University of California, Davis, California 95616*

(Received 18 December 1996)

We study the magnetic phase diagram of a one-dimensional, orbitally degenerate Hubbard model using the Lanczos algorithm to project out the ground state. Using lattices larger than those previously explored with diagonalization approaches, we find a phase diagram which is in much better agreement with a strong coupling analysis. In addition to determining the phase diagram by calculating the spin sector of minimum energy, we also show results for the spin-spin correlations and participation ratio, which further characterize the magnetic order and the itinerancy of the electrons. We then describe results for the case when the intersite hybridization is different for the two orbitals. [S0163-1829(97)04818-2]

### I. INTRODUCTION

The spontaneous breaking of rotational symmetry to a ferromagnetic state is a difficult problem in statistical physics. Nevertheless, the occurrence of a ferromagnetic transition is well established in spin models like the Ising,  $XY$ , and Heisenberg Hamiltonians, when the dimension is sufficiently high, and indeed a combination of analytic and numerical work has quantitatively characterized the details of the order of the transitions, the critical temperature, and critical exponents.<sup>1</sup> However, many ferromagnets, like the transition metals, are not well described by such spin systems. Instead, their transport properties exhibit features which can only be understood within the context of a band model where the electrons are delocalized. While calculations within the local spin density approximation have yielded important insights,<sup>2,3</sup> the precise nature of the correlations responsible for such itinerant ferromagnets is still an open issue.

For such itinerant ferromagnets, an alternate to electronic structure calculations is to study correlation effects giving rise to magnetism in tight binding Hamiltonians.<sup>1,4,5</sup> The simplest such model, the single-band Hubbard Hamiltonian, consists of one orbital hybridized with near neighbor hopping  $t$ , and an on-site repulsion  $U$  between electrons of opposite spin. The existence of an *antiferromagnetic* regime near half-filling is well established by a number of numerical and analytic techniques.<sup>6</sup> The single band Hubbard Hamiltonian also exhibits a ferromagnetic phase at large  $U/t$  within mean field theory. Unlike antiferromagnetism, this phase has not been observed numerically, and hence there is much less certainty concerning the validity of this Hartree-Fock prediction of ferromagnetism than its antiferromagnetic counterpart.

What is rigorously known concerning ferromagnetism? Nagaoka established that in the limit of infinite  $U/t$ , the state with a single hole doped into half-filling is ferromagnetic.<sup>7</sup> The question of extending this result to finite hole density has been addressed recently in a number of papers,<sup>8</sup> and it is currently known<sup>9</sup> that ferromagnetism is unstable for doping  $\delta > \delta_c = 0.25$  and interactions  $U < U_c = 78t$ . That an interaction strength an order of magnitude greater than the bandwidth,  $W = 8t$ , is necessary for ferromagnetism is indicative

of the difficulty with which the single band model supports spin alignment.

There are also additional rigorous results pertaining to ferromagnetism in the Hubbard model. The Lieb-Mattis theorem rules out ferromagnetism in the one-dimensional (1-D) Hubbard model.<sup>10</sup> That the 2D Hubbard model cannot exhibit long range magnetic order at finite temperature is a consequence of the Mermin-Wagner theorem.<sup>11,12</sup> Ferromagnetism has been established in lattices with flat bands, especially those arising on bipartite lattices with different numbers of sites on the two sublattices.<sup>13-15</sup> Besides these renewed studies of the simplest Hubbard model, a number of recent papers have focused on the effect of including additional off-diagonal interactions such as bond-charge and exchange terms.<sup>16-18</sup>

The suggestion that orbital degeneracy plays a crucial role in itinerant ferromagnetism, a view supported at the most primitive level by the observation that ferromagnetism occurs most frequently in metals with  $d$  and  $f$  electrons, has a history beginning with Van Vleck<sup>19</sup> and Slater, Slater, and Koster.<sup>20</sup> This picture was refined by Roth,<sup>21</sup> Kugel and Khomski,<sup>22</sup> and Cyrot and Lyon-Caen,<sup>23</sup> who emphasized the simultaneous appearance of orbital ordering in which the occupation of the orbitals alternates, along with ferromagnetism. This analytic work was within the random phase approximation and mean field theory applied to strong coupling versions of the model. Many of the essential features of the picture were verified by exact diagonalization and Monte Carlo studies of Gill and Scalapino.<sup>24</sup> However results from diagonalization of small clusters and strong coupling arguments were only qualitatively in agreement.

In this paper we will explore this specific issue of ferromagnetism arising within a multi-orbital Hubbard Hamiltonian with a Hund's rule coupling. In particular, we will extend the numerical work of Gill and Scalapino to larger lattices and resolve the disagreement between cluster and strong coupling calculations. We will also present new results showing how the participation ratio can distinguish the phases on the two sides of the ferromagnetic region. Finally, we will determine the phase diagram in limits where the intersite hybridization is different for the two orbitals, as would occur, for example, in a multiband model consisting of extended and localized orbitals. The organization of this

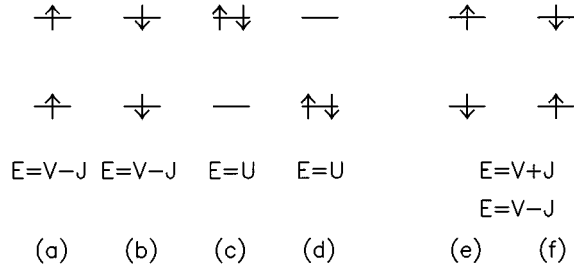


FIG. 1. The six possible states  $|n_{\lambda s}\rangle$  of two electrons on one site (with two orbitals). The first four states are not connected by  $H$  to any other states, if  $t=0$ , and the energy listed below each state is the diagonal part of  $H$ ,  $\langle n_{\lambda s}|H|n_{\lambda s}\rangle$ . The last two states are connected to each other by the Hund's rule coupling  $J$ , and the energies listed below them are the two possible eigenenergies.

paper is as follows: In Sec. II we write down the Hamiltonian and discuss its strong coupling limit and also the computational approach we use. In Sec. III we present results for the symmetric case where the hopping of electrons between sites in each orbital is identical, and in Sec. IV we take up the situation where one set of orbitals is more localized than the other. Section V contains some concluding remarks.

## II. MODEL AND COMPUTATIONAL APPROACH

We consider a specific Hamiltonian which incorporates orbital degeneracy and Hund's rule coupling,

$$\begin{aligned}
 H = & -t \sum_{i,\lambda,s} (d_{i+1\lambda s}^\dagger d_{i\lambda s} + d_{i\lambda s}^\dagger d_{i+1\lambda s}) + U \sum_{i\lambda} n_{i\lambda\uparrow} n_{i\lambda\downarrow} \\
 & + V \sum_{i s s'} n_{i1s} n_{i2s'} - J \sum_{i s s'} d_{i1s}^\dagger d_{i1s'} d_{i2s}^\dagger d_{i2s}. \quad (1)
 \end{aligned}$$

Here  $d_{i\lambda s}$  ( $d_{i\lambda s}^\dagger$ ) are destruction (creation) operators for fermions of spin  $s$  at site  $i$  and in orbital  $\lambda=1,2$ .  $t$  is an intersite hybridization between sites in a 1D chain. We set  $t=0.25$ , so that the bandwidth  $W=4t=1$  is our scale of energy.  $U$  is an on-site repulsion between electrons of opposite spin on the same site and in the same orbital.  $V$  represents the on-site interorbital repulsion. Finally,  $J$  is a Hund's rule coupling. Note that, as written,  $J$  contains a spin diagonal term which is an attractive interaction between electrons on different orbitals. Thus we require  $V>J$  so the total interorbital interaction is repulsive. Besides the parameters in the Hamiltonian, the physics is also determined by the filling per site  $\langle n \rangle$  and the temperature  $T$ . In this paper we will be concerned with ground state properties,  $T=0$ , and will also focus on quarter-filling  $\langle n \rangle=1$ . While systems of higher dimensionality are clearly the ones of most interest, we can nevertheless get significant insight into the effect of the various interactions even in 1D.

It is useful to consider the case  $t=0$  since this is the starting point for a strong coupling analysis and also since certain relationships between the interaction parameters  $U, V, J$  are most clearly evident. For  $t=0$  the Hamiltonian describes a set of decoupled sites. Let us consider a site with two electrons. The six possible configurations, and their associated energies, are shown in Fig. 1. If  $S_z = \pm 1$ , that is the

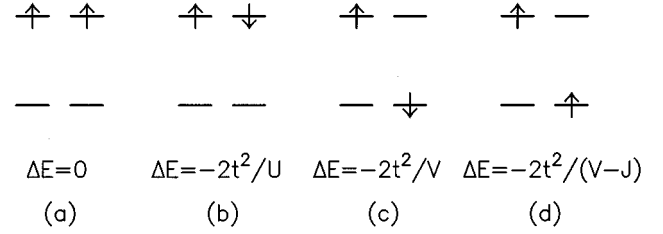


FIG. 2. Some of the possible configurations of neighboring singly occupied sites. The second-order lowering of energy due to  $t$  is indicated. The lowest energy is associated with a ferromagnetic spin configuration with opposite orbitals being occupied on the two adjacent sites.

electron spins are parallel, then the energy is  $V-J$ , which is positive since we require  $V>J$ . If  $S_z=0$ , the electron spins are antiparallel, and the energies are  $U$  (with a degeneracy of 2), and  $V \pm J$ . The  $S_z=0$  state with energy  $V-J$  is the third component of the spin-one triplet together with the  $S_z = \pm 1$  states. The two possible choices of orbital quantum number can be considered as a pseudospin  $\frac{1}{2}$ . Then the three remaining states, two of energy  $U$ , and one of energy  $V+J$ , form the ‘‘orbital’’ triplet  $L=1$ . Orbital symmetry thus requires  $U=V+J$ .

The key point of this single-site analysis is that the Hund's rule coupling  $J$  favors ‘‘atomic ferromagnetism,’’  $S=1$ , that is alignment of the moments of two electrons on the same site. We are, however, interested in the ‘‘quarter-filled’’ case,  $\langle n \rangle=1$ . In such a situation where there is on average a single electron per site, at  $t=0$  all levels are degenerate. We can, however, put two such singly occupied sites adjacent to each other and analyze the energy to second order in the hopping  $t$  (Fig. 2). Such an analysis is what leads to the conclusion that antiferromagnetic correlations are dominant in the single-band Hubbard model at half filling, and to the familiar strong coupling treatment based on the spin-1/2 antiferromagnetic Heisenberg Hamiltonian. However, in the case of the orbitally degenerate model, the situation is more complicated, and ferromagnetism with orbital ordering is favored, as seen in Fig. 2.

This observation that ferromagnetism is associated with the formation of an orbital superlattice was first made by Roth<sup>21</sup> and formalized by Cyrot and Lyon-Caen,<sup>23</sup> and also by Kugel and Khomskii.<sup>22</sup> One introduces a ‘‘pseudospin’’ operator  $L$  with the property that  $L^+$  takes a fermion in orbital 2 and transports it to orbital 1,  $L^-$  takes a fermion in orbital 1 and transports it to orbital 2, and  $L^z = \pm \frac{1}{2}$  for fermions in orbitals 1 and 2, respectively. Then the Hamiltonian Eq. (1) can be written at strong coupling as

$$\begin{aligned}
 H_{\text{eff}} = & \sum_i \frac{4t^2}{U} (\vec{S}_i \cdot \vec{S}_{i+1} - \frac{1}{4}) (L_i^z L_{i+1}^z + \frac{1}{4}) \\
 & + \frac{2t^2}{V-J} (\vec{S}_i \cdot \vec{S}_{i+1} + \frac{3}{4}) (\vec{L}_i \cdot \vec{L}_{i+1} - \frac{1}{4}) \\
 & - \frac{2t^2}{V+J} (\vec{S}_i \cdot \vec{S}_{i+1} - \frac{1}{4}) [L_i^z L_{i+1}^z - \frac{1}{4} \\
 & - \frac{1}{2} (L_i^+ L_{i+1}^- + L_i^- L_{i+1}^+)]. \quad (2)
 \end{aligned}$$

Gill and Scalapino have studied this strong coupling model with a quantum Monte Carlo method.<sup>24</sup> A similar model has recently been used in order to understand the magnetic properties of  $C_{60}$ .<sup>25</sup>

While considerable understanding of the original itinerant electron Hamiltonian, Eq. (1), can be gained by considering this strong coupling  $H_{\text{eff}}$ , a standard approach to the opposite, weak coupling, limit is the RPA. In the case of the single-band model, the resulting ‘‘Stoner criterion’’ is that a magnetic instability occurs at  $U\chi_0(q)=1$ . Near half-filling,  $\chi_0(q)$  is largest at momentum  $q=\pi$ , that is, antiferromagnetic order is expected. Indeed, for a square lattice in two dimensions,  $\chi_0(\pi, \pi)$  diverges as  $T\rightarrow 0$  [ $\ln^2(T)$ ] indicating that antiferromagnetic order exists all the way down to  $U=0$ . For other fillings, at large  $U$ , the uniform susceptibility  $\chi(0)$  is largest. At zero temperature  $\chi_0(0)=N(\epsilon_F)$  and the Stoner condition for ferromagnetism is  $UN(\epsilon_F)=1$ . In the model with  $m$  degenerate orbitals, the analogous criterion for magnetic ordering is  $[U+(m-1)J]N(\epsilon_F)=1$ . Thus within this weak coupling treatment it is also apparent that the Hund’s rule coupling favors ferromagnetism by allowing ordering at a lower  $U$ .

Results in the intermediate coupling regime require other analytic or numerical methods. Our calculational approach is Lanczos diagonalization.<sup>26</sup> This technique and its variants have been widely used recently to study the properties of correlated electron systems on small clusters, especially those models which cannot be easily analyzed using the quantum Monte Carlo method. The Lanczos algorithm involves the explicit application of the Hamiltonian to states in the Hilbert space. CPU time and storage grow exponentially with system size. Here we report on studies of four- and six-site, two-orbital, quarter-filled systems where the maximal Hilbert space dimension  $D$ , exploiting certain symmetries of  $H$ , is  $D=48\,400$ . Eight-site systems would have a Hilbert space of dimension exceeding 3.3 million.

The Lanczos algorithm provides the ground state energy  $E_0$  and wave function  $|\psi_0\rangle$ . We will infer the nature of  $|\psi_0\rangle$  through a number of different measurements. First, by calculating the energy in different sectors of total  $S_z$ , we can determine whether the ground state is ferromagnetic. Specifically, if the ground state energies obtained by restricting to different sectors of total  $S_z$  are degenerate, then this means that  $|\psi_0\rangle$  has nonzero total spin, a ferromagnet. The reason is that the Lanczos algorithm gives the energy of the lowest state not orthogonal to the starting wave function. Since the total  $S_z$  commutes with  $H$ , a starting wave function of total  $S_z$  nonzero will have no overlap with the ground state unless the ground state has nonzero spin. On the other hand, if the ground state is not a singlet, different total  $S_z$  starting wave functions will typically overlap the ground state, and all will yield the identical  $E_0$  after the Lanczos iterations.

The nature of the ground state can also be inferred by measuring the participation ratio,

$$\mathcal{P}=1/\sum_i |\psi_0(i)|^4. \quad (3)$$

Here  $\psi_0(i)$ ,  $i=1, \dots, D$ , are the  $D$  components of the wave function in the basis we have chosen for the Hilbert space. If not many components are nonzero, for example if  $|\psi_0\rangle$  is

dominated by a few magnetically ordered configurations, then  $\mathcal{P}$  will be relatively small. On the other hand, in a disordered, itinerant phase, we expect  $\mathcal{P}$  to be large.<sup>27</sup>

We can also explicitly measure the spin-spin correlations and their Fourier transform, the structure factor,

$$c(j)=\langle \psi_0 | s_z(l) s_z(l+j) | \psi_0 \rangle,$$

$$S_{zz}(q)=\sum_j c(j) e^{iqj}. \quad (4)$$

Here  $s_z(l)=n_{l1\uparrow}-n_{l1\downarrow}+n_{l2\uparrow}-n_{l2\downarrow}$  is the total  $z$  component of spin, including both orbitals. We expect  $c(j)$  to be positive for different separations  $j$  in a ferromagnetic phase, to alternate in sign in an antiferromagnetic phase, and to be ‘‘small’’ as  $j$  increases in a disordered, paramagnetic state. We expect the structure factor  $S_{zz}(q=0)$  to become large in the ferromagnetic phase, while an increase in  $S_{zz}(q=\pi)$  will signal antiferromagnetism. Of course in one dimension, we do not expect any true long range order. To analyze the nature of the ground state in detail would require studies of large lattices and a determination of the exponent describing the power law of the decay of  $c(j)$  and other correlation functions.<sup>28</sup> Here we shall confine ourselves to examining the qualitative behavior of  $c(j)$ , for example the sign of the near neighbor correlations. However, we shall find this agrees well with the nature of the phase diagram inferred from the energy and participation ratio.

### III. RESULTS: SYMMETRIC HOPPING

We first present results for the case when the hopping parameter  $t$  is the same for each type of orbital. All data in this and the following section are for six sites, unless otherwise indicated.

In Fig. 3(a) we show the ground state energy in different sectors  $n_\uparrow - n_\downarrow$  of total  $S_z$ . We observe there a range of Hund’s rule couplings,  $J_{c1} < J < J_{c2}$  where the different sectors have the same ground state energies. As remarked in the previous section, such a degeneracy is a signature of a ferromagnetic ground state with total spin  $S \neq 0$ .

We can get further insight into the nature of the ground state by examining the sign of the near neighbor spin-spin correlation function.  $c(1) < 0$  is characteristic of an antiferromagnetic phase, while  $c(1) > 0$  is characteristic of ferromagnetism. In Fig. 4 we see that  $c(1)$  is negative for  $J < J_{c1}$  and positive for  $J_{c1} < J < J_{c2}$ . Finally,  $c(1) \approx 0$  for  $J > J_{c2}$ , suggesting a weakly ordered, paramagnetic phase. The behavior of the structure factor (not shown) is consistent with this. For  $J < J_{c1}$ , the structure factor  $S(q)$  is peaked at momentum  $q=\pi$ , while it is peaked at momentum  $q=0$  in the intermediate region  $J_{c1} < J < J_{c2}$ . Of course, the local spin correlation only contains qualitative information. We need to exhibit the behavior of  $c(l)$  as  $l \rightarrow \infty$ , or perform a scaling analysis of the structure factor, before rigorously determining the nature of the dominant correlations in the system. Such detailed analysis is not possible for the system sizes considered here.

We next consider the behavior of the participation ratio. As we have discussed,  $\mathcal{P}$  measures the number of different states in our basis which have a significant component in the

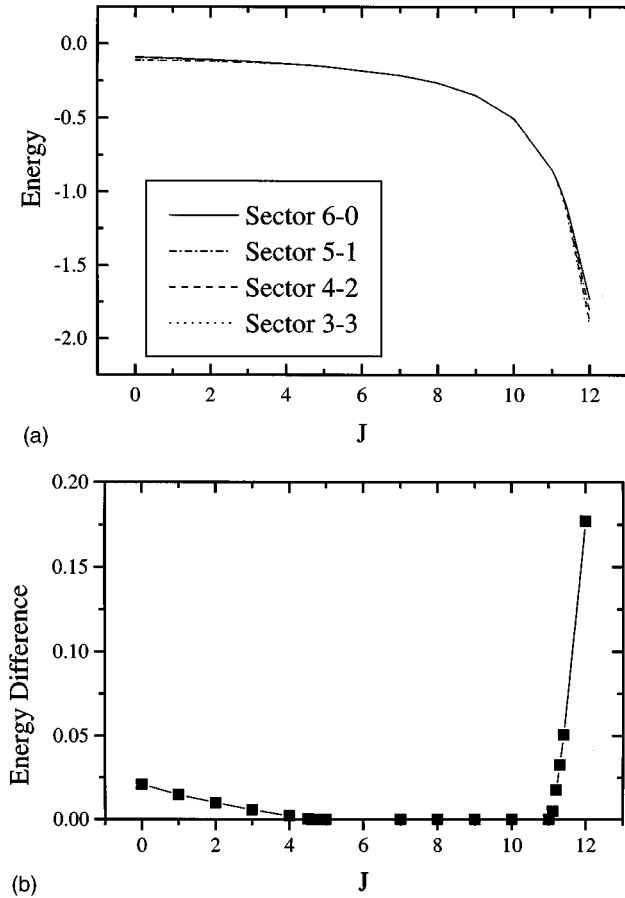


FIG. 3. (a) The ground state energy per site as a function of Hund's rule coupling  $J$  for different total  $S_z$ . Here  $V/4t=12$  and  $U=V+J$ . (b) The same as (a) except the difference in energies between the 6-0 and 3-3 sectors is shown. When  $\Delta E_0=0$ , the ground state is ferromagnetic.

expansion of  $|\psi_0\rangle$ . Since we work in a basis of eigenstates of the occupation numbers, perfectly ferromagnetic or antiferromagnetic states can be represented by a single basis vector and hence  $\mathcal{P}=1$ . Of course, the existence of quantum fluctuations in the form of the nonzero hopping parameter  $t$  precludes that these be eigenstates of the Hamiltonian. Nevertheless we expect that  $\mathcal{P}$  might remain small for magnetically ordered phases. On the other hand, an itinerant phase will be characterized by a much larger number of basis vectors contributing to the construction of the ground state. This expectation is borne out in Fig. 5, where we see that  $\mathcal{P}$  is small both for  $J < J_{c1}$ , the region which the measurement of  $c(1)$  suggested might be antiferromagnetic, and for  $J_{c1} < J < J_{c2}$ , the region that both  $E_0$  degeneracies and  $c(1)$  suggested might be ferromagnetic. For a value  $J > J_{c2}$  consistent with that determined in Figs. 3 and 4, the participation ratio rises abruptly.

All three measurements, the ground state energy, spin correlations, and participation ratios give consistent locations for two critical values of the Hund's rule coupling  $J$  where magnetic transitions occur. We can put together sweeps of  $J$  at different values of  $V$  to construct a phase diagram. For weak coupling, no magnetic order occurs, but for  $V/4t$  large there exists a ferromagnetic region. This region is exhibited for a four-site lattice in Fig. 6(a), along with the strong cou-

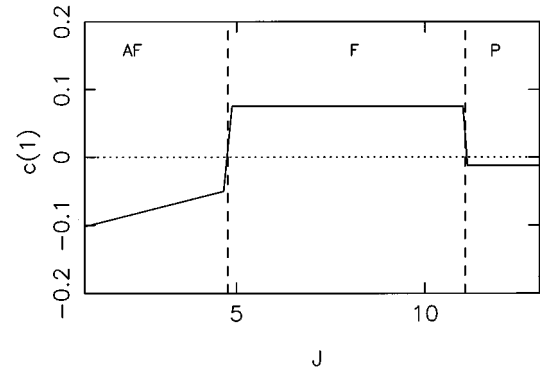


FIG. 4. The near neighbor spin-spin correlation function  $c(1)$  as a function of Hund's rule coupling  $J$ . Here  $V/4t=12$  and  $U=V+J$ .  $c(1)$  is negative (antiferromagnetic) for  $J < J_{c1}$ , positive (ferromagnetic) for  $J_{c1} < J < J_{c2}$ , and relatively small (paramagnetic) for  $J > J_{c2}$ . The values  $J_{c1}=4.8$  and  $J_{c2}=11.1$  which bound the ferromagnetic region are in good agreement with the energy degeneracy measurement of Fig. 3 (vertical dashed lines).

pling phase boundaries. As discussed by Gill,<sup>24</sup> the lower phase boundary is obtained by equating the energies of the ferromagnetic configuration of Fig. 2(d) with the sum of the antiferromagnetic energies of Figs. 2(b) and 2(c). This gives the condition  $J=V^2/(U+V)$ , which along with  $U=V+J$  yields the lower phase boundary  $J_{c1}=(\sqrt{2}-1)V$  of Figs. 6(a) and 6(b). Ferromagnetism becomes unstable to a disordered phase when the energy  $V-J$  which induces moment formation by preventing double occupation of a site [Figs. 1(a) and 1(b)], becomes of order the bandwidth  $4t$ . This yields the upper boundary  $J=V-4t$  of Figs. 6(a) and 6(b).

The four-site calculation, originally done by Gill<sup>24</sup> and reproduced by us, agrees qualitatively with the strong coupling analysis. However, as shown in Fig. 6(b), the agreement is much improved if a six-site cluster is considered, as we have done here. It would be interesting to do the calculation for a yet larger eight-site cluster to ensure that the agreement remains good.

We can also perform the calculation for a case when the

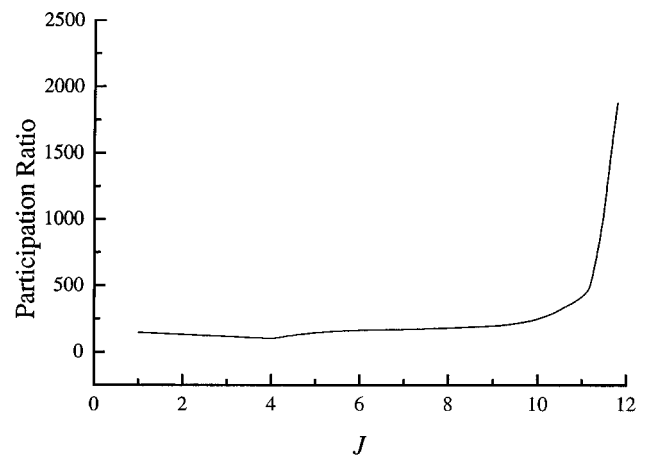
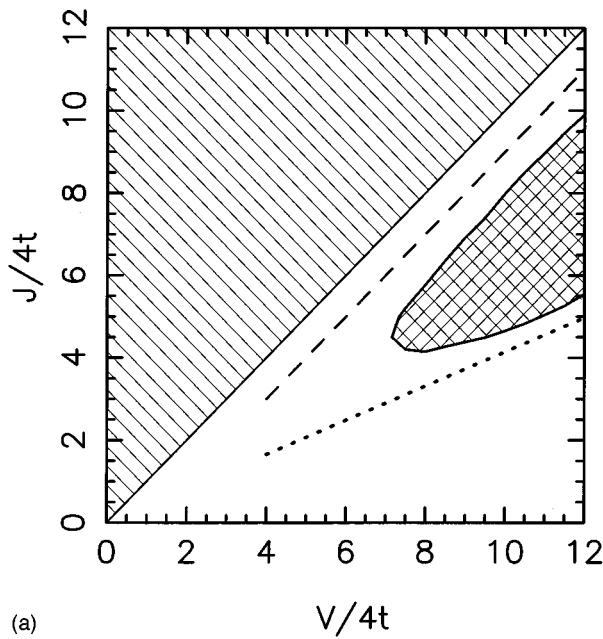
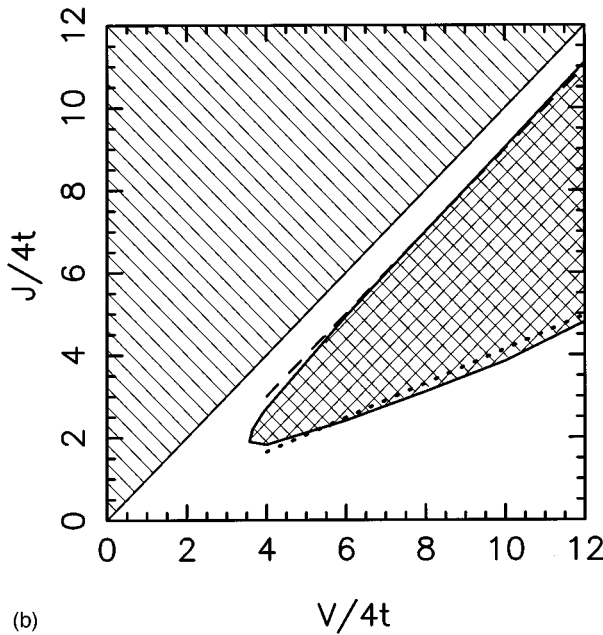


FIG. 5. The participation ratio as a function of Hund's rule coupling  $J$ . Here  $V/4t=12$  and  $U=V+J$ . In the magnetically ordered phases,  $\mathcal{P}$  is small.  $\mathcal{P}$  increases dramatically in the paramagnetic phase.



(a)



(b)

FIG. 6. The ground state phase diagram inferred from the data of Figs. 3–5. The shaded region of  $J > V$  is physically forbidden. The hatched region is ferromagnetic. The dotted and dashed lines are the strong coupling boundaries. (a) Four sites. (b) Six sites. Our four-site phase diagram is identical to that obtained by Gill and Scalapino using diagonalization. The six-site phase diagram represents a significant improvement of agreement with the strong coupling calculation.

repulsion for electrons of opposite spin on the same site and orbital is infinite. In this case, as shown in Fig. 7, the region of ferromagnetism is considerably enhanced, but the agreement with the cluster and strong coupling calculations remains good.

#### IV. RESULTS: ASYMMETRIC HOPPING

Here we present results for the case when the intersite hybridization  $t$  depends on  $\lambda$ , as might occur, for example, if

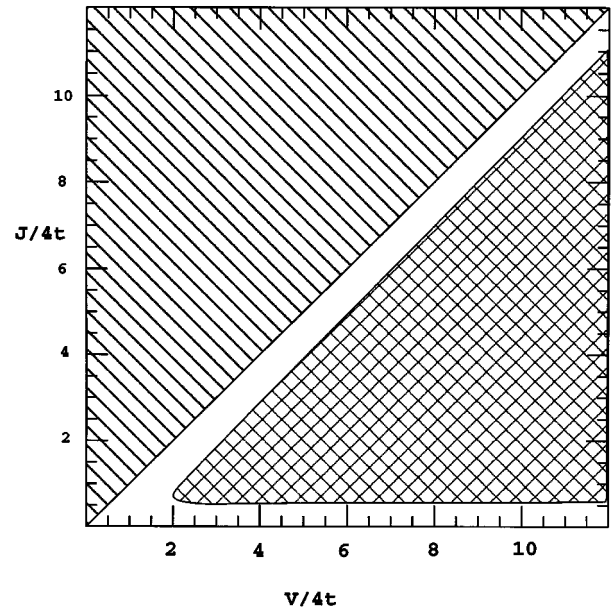


FIG. 7. The regime of ferromagnetism for  $U = \infty$ . The lower strong coupling phase boundary would be at  $J/4t = 0$ .

orbital  $\lambda = 1$  comprised an extended conduction band, and  $\lambda = 2$  a set of localized orbitals. Such different choices of  $t_\lambda$  are, of course, considered in the “Anderson lattice” Hamiltonian. (However in that model there is an interorbital hybridization on each site, as opposed to the interorbital repulsion and Hund’s rule coupling considered here, and the dominant magnetic ordering is antiferromagnetic.) Figures 8(a) and 8(b) show the regions of ferromagnetism for cases when the orbitals  $\lambda = 2$  do not hybridize at all,  $t_2 = 0$ , and when the hybridization  $t_2 = 0.5t_1$ .

Results for  $J_{c1}$  and  $J_{c2}$  for  $V = 12$  and a range of values of  $t_2/t_1$  are given in Fig. 9. The ferromagnetic region expands somewhat at the expense of antiferromagnetic order as  $t_2$  is turned on from zero, the position of  $J_{c1}$  shifting by about 25%. We can understand this by a slight generalization of strong coupling analysis of Gill and Scalapino to include different hopping parameters in the diagrams of Figs. 2(b)–2(d). If  $t_2 = \alpha t_1$  we find  $J_{c1}/V = [\sqrt{1 + \alpha^2} - 1]/\alpha^2$ . This analysis predicts about a 20% decrease in  $J_{c1}$  from  $\alpha = 0$  to  $\alpha = 1$ , in reasonable agreement with the numerical work.

Meanwhile, the upper ferromagnetic-paramagnetic boundary  $J_{c2}$  is even less sensitive to the hybridization  $t_2$ , shifting only by 5% or so as  $t_2$  varies from describing completely localized orbitals to a hybridization equal to  $t_1$ . This is easily understood since the orbital  $\lambda = 1$  bandwidth remains fixed at  $W_1 = 4t$  and can drive the destruction of the moments independent of the value of the bandwidth  $W_2$  of the second orbital  $\lambda = 2$ .

#### V. CONCLUSIONS

In this paper we have determined the phase diagram of an orbitally degenerate tight binding Hamiltonian which includes both intra- and interorbital repulsions and a Hund’s rule coupling. We have shown that the previous agreement between diagonalization and strong coupling calculations

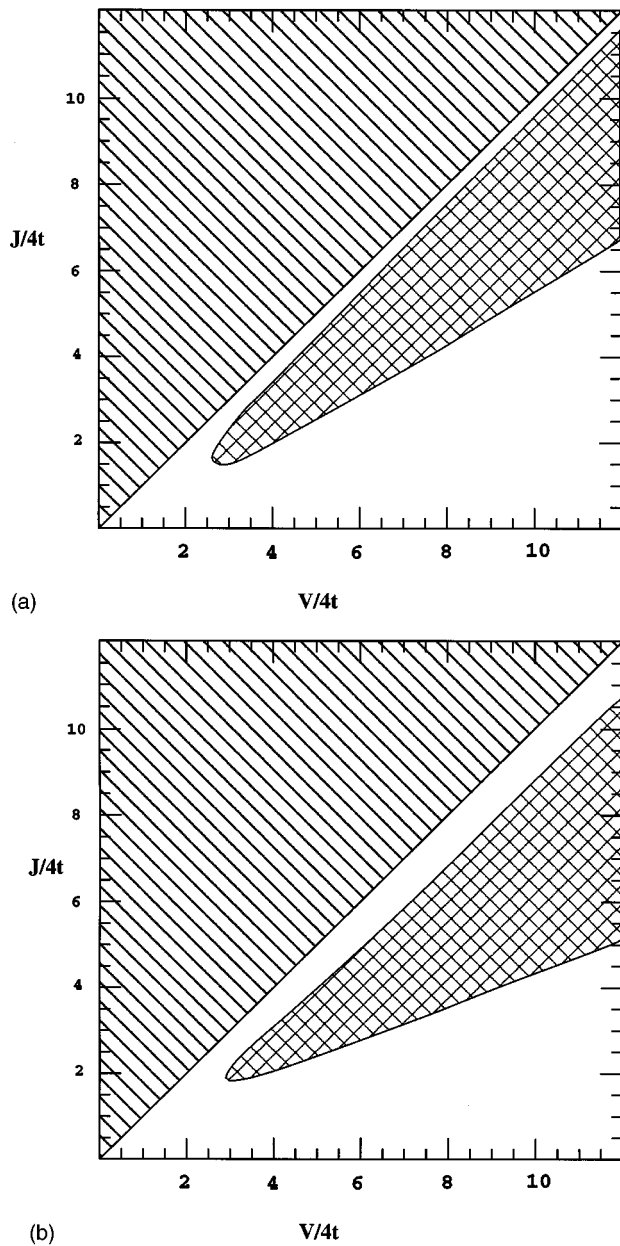


FIG. 8. The phase diagram showing the regime of ferromagnetism for (a)  $t_1=1$ ,  $t_2=0.0$ , and (b)  $t_1=1$ ,  $t_2=0.5$ . The symmetric case  $t_1=t_2=1$  was shown in Fig. 2(b). The size of the ferromagnetic region is not very sensitive to different choices of  $t_2$ .

can be significantly improved by calculations on larger clusters. We have also shown that an appropriately defined participation ratio can be used to identify the critical couplings for a transition into a disordered phase.

We have presented calculations for a generalized version of the Hamiltonian which allows for intersite hybridizations

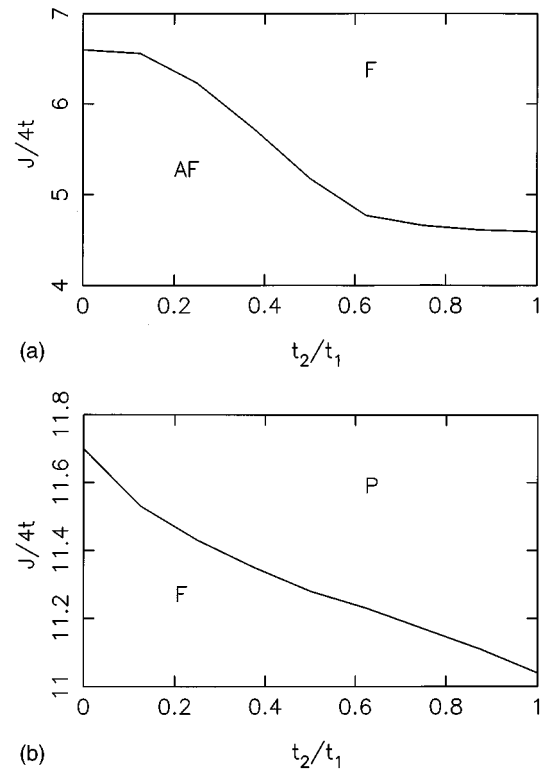


FIG. 9. (a) The value of the Hund's rule term  $J_{c1}$  which gives the lower phase boundary of the ferromagnetic region as a function of  $t_2$ . We see  $J_{c1}$  is largest, that is, the antiferromagnetic region is expanded at the expense of ferromagnetism, at  $t_2=0$ . (b) The value of the Hund's rule term  $J_{c2}$  which gives the upper phase boundary of the ferromagnetic region as a function of  $t_2$ . The paramagnetic phase expands slightly at the expense of ferromagnetism as  $t_2$  increases, but the effect is relatively small.

which differ for the two orbitals. Our conclusion is that the regime of ferromagnetism is only weakly dependent on the ratio  $t_2/t_1$  and we present generalizations of existing strong coupling calculations to explain this behavior.

It would be interesting to extend these calculations to yet larger lattices. Unfortunately, this cannot be done for the original itinerant electron Hamiltonian with either world-line or determinant quantum Monte Carlo methods, owing to the "sign" problems. Likewise, the spin-only strong coupling version has a sign problems within a world-line approach, and has only been simulated in a "self-consistent mean field treatment."<sup>24</sup> It is probably possible to attack larger lattices using the "density matrix renormalization group."<sup>29</sup>

#### ACKNOWLEDGMENTS

This work was supported by Grant No. NSF-DMR-9528535 and the Associated Western Universities.

\*Permanent address: Rockwell International Corporation, 4311 Jamboree Road, Newport Beach, CA 92660.

<sup>1</sup>D. C. Mattis, *The Theory of Magnetism I* (Springer-Verlag, Berlin, 1981), and references cited therein.

<sup>2</sup>W. L. Moruzzi, A. R. Williams, and J. F. Janak, *Calculated Elec-*

*tronic Properties of Metals* (Pergamon, New York, 1978).

<sup>3</sup>C. Wang, B. M. Klein, and H. Krakauer, *Phys. Rev. Lett.* **54**, 1852 (1985).

<sup>4</sup>C. Herring, in *Magnetism*, edited by G. T. Rado and H. Suhl (Academic, New York, 1966), Vol. IV.

- <sup>5</sup>R. Strack and D. Vollhardt, *J. Low Temp. Phys.* **99**, 385 (1995).
- <sup>6</sup>*The Hubbard Model*, edited by A. Montorsi (World Scientific, Singapore, 1992).
- <sup>7</sup>Y. Nagaoka, *Phys. Rev.* **147**, 392 (1966).
- <sup>8</sup>B. S. Shastry, H. R. Krishnamurthy, and P. W. Anderson, *Phys. Rev. B* **41**, 2375 (1990); A. G. Basile and V. Elser, *ibid.* **41**, 4842 (1990); W. von der Linden and D. M. Edwards, *J. Phys. Condens. Matter* **3**, 4917 (1991); Th. Hanisch and E. Muller-Hartmann, *Ann. Phys. (Leipzig)* **2**, 381 (1993).
- <sup>9</sup>P. Wurth, G. Uhrig, and E. Mueller-Hartmann, *Ann. Phys. (Leipzig)* **5**, 148 (1996).
- <sup>10</sup>E. H. Lieb and D. Mattis, *Phys. Rev.* **125**, 164 (1962).
- <sup>11</sup>D. Ghosh, *Phys. Rev. Lett.* **27**, 1584 (1971).
- <sup>12</sup>N. D. Mermin and H. Wagner, *Phys. Rev. Lett.* **17**, 1133 (1966).
- <sup>13</sup>E. H. Lieb, *Phys. Rev. Lett.* **62**, 1201 (1989).
- <sup>14</sup>A. Mielke, *J. Phys. A* **24**, 3311 (1991).
- <sup>15</sup>H. Tasaki, *Phys. Rev. Lett.* **69**, 1608 (1992).
- <sup>16</sup>D. K. Campbell, J. T. Gammel, and E. Y. Loh, *Phys. Rev. B* **38**, 12 043 (1988).
- <sup>17</sup>J. E. Hirsch, *Phys. Rev. B* **40**, 2354 (1989).
- <sup>18</sup>M. Kollar, W. R. Strack, and D. Vollhardt, *Phys. Rev. B* **53**, 9225 (1996).
- <sup>19</sup>J. H. Van Vleck, *Rev. Mod. Phys.* **25**, 220 (1953).
- <sup>20</sup>J. C. Slater, H. Statz, and G. F. Koster, *Phys. Rev.* **91**, 1323 (1953).
- <sup>21</sup>L. M. Roth, *Phys. Rev.* **149**, 306 (1966).
- <sup>22</sup>K. I. Kugel and D. I. Khomskii, *Sov. Phys. JETP* **37**, 725 (1974).
- <sup>23</sup>M. Cyrot and C. Lyon-Caen, *J. Phys. (Paris)* **36**, 253 (1975).
- <sup>24</sup>W. Gill and D. J. Scalapino, *Phys. Rev. B* **35**, 215 (1987).
- <sup>25</sup>D. P. Arovas and A. Auerbach, *Phys. Rev. B* **52**, 10 114 (1995).
- <sup>26</sup>See E. Dagotto and A. Moreo, *Phys. Rev. D* **31**, 865 (1986); E. Gagliano, E. Dagotto, A. Moreo, and F. Alcaraz, *Phys. Rev. B* **34**, 1677 (1986); **35**, 5297 (1987), and references cited therein.
- <sup>27</sup>Note that  $P$  does *not* measure the number of real space sites participating in the state, but the number of states in the Hilbert space contributing to the ground state wave function. In studies of noninteracting models, such as the Anderson Hamiltonian, it happens that the basis vectors are site occupation vectors, so measuring the number of states contributing *is* equivalent to measuring the real space extent of  $|\psi_0\rangle$ .
- <sup>28</sup>For examples of this sort of analysis see, for example, R. M. Noack, S. R. White, and D. J. Scalapino, *Phys. Rev. Lett.* **73**, 882 (1994); A. W. Sandvik, D. J. Scalapino, and C. Singh, *Phys. Rev. B* **48**, 2112 (1993).
- <sup>29</sup>S. R. White, *Phys. Rev. Lett.* **69**, 2863 (1992).